10636 *Macromolecules* **2010**, *43*, 10636–10644
DOI: 10.1021/ma102251e

Macromolecules
ARTICLE

Novel Approach to Controllable Synthesis of Gold Nanoparticles Supported on Polyaniline Nanofibers

Jie Han, Liya Li, and Rong Guo*

School of Chemistry and Chemical Engineering, Yangzhou University, Yangzhou, 225002, Jiangsu, P. R. China

Received September 30, 2010; Revised Manuscript Received November 14, 2010

ABSTRACT: A facile and effective route has been proposed to synthesize gold nanoparticles with controllable size that uniformly deposited on surfaces of polyaniline (PANI) nanofibers, where PANI nanofibers themselves act as both supporter and reductant. Effects of reagent concentration, reaction time, and temperature on size and uniformity of gold nanoparticles are investigated. Furthermore, a functional doping acid of typical thioglycolic acid (TA) that introduced in PANI nanofibers shows good potential for improvement in uniformity of composites and control over gold nanoparticle size. Fourier transform infrared (FTIR), X-ray diffraction (XRD), and ultraviolet−visible (UV−vis) spectra are used to characterize PANI nanofiber/gold nanoparticle composites. Adaptability of this approach for making PANI nanofiber composites with other noble metal nanoparticles, such as platinum, silver, and palladium nanoparticles, is also studied. A possible formation mechanism involved has been then proposed. Furthermore, PANI nanofiber/gold nanoparticle composites are found to serve as effective recycled catalysts to activate the reduction of 4-nitrophenol (4NP) in the presence of $NaBH_4$, where size of gold nanoparticles is found to play the determining role on catalytic activity.

1. Introduction

Conducting polymer of polyaniline (PANI) possesses advantages of reversible doping/dedoping process, special redox chemistry, easy of synthesis, and low cost and therefore generates numerous interests in the past few years.[1,2] Nanostructured synthesis and applications of PANI are the research focus in recent years.[3,4] Among various morphologies, PANI nanofibers have been thoroughly investigated due to the intrinsic one-dimensional structures of PANI rigid molecule. Scalable and reproducible synthesis of uniform PANI nanofibers and formation mechanisms involved have been well-documented.[5−7] In comparison with conventional bulk and other morphologies of PANI, PANI nanofibers show good suspension ability, high surface areas, and low-dimensional systems that endow then with improved performances for applications such as chemical sensors.[8−10]

Recently, composites of PANI and noble metal nanoparticles have generated considerable interest related to their vast potentials in memory devices,[11] catalysts,[12−15] and sensors.[16−18] Synthesis of such composites has been realized by blending PANI with noble metal nanoparticles earlier.[19] In this method, PANI and noble metal nanoparticles have to be both synthesized in advance, and uniform composites with highly dispersed noble metal nanoparticles are hard to achieve. Recent reports show that PANI or its derivatives also show good redox activities toward some noble metal ions, such as Ag(I), Au(III), Pd(II), or Pt(IV), which give the opportunity for making PANI/noble metal nanoparticle composites by simply mixing PANI and noble metal salt together.[11−14,20−24] In most of the cases, it is believed that emeraldine base form of PANI is oxidized to pernigraniline base form of PANI; that is, benzenoid rings of PANI have been oxidized to quinonoid rings. It is reported that dedoped PANI nanofibers can be regard as reactive support for gold and palladium nanoparticles, and their applications as memory devices and catalysts have been investigated.[10,11] More recent, HCl-doped PANI nanofibers also show redox activity toward gold ions and application of as-formed gold nanoparticles decorated PANI nanofibers for H_2O_2 sensing is studied.[25] In addition, HCOOH-doped PANI nanofibers are also used as reactive supporter for deposition platinum nanoparticles, and further use as nanoelectrocatalysts for electrochemical devices is investigated.[26] However, successful synthesis of noble metal nanoparticles that uniformly supported on PANI nanofibers and control over size of noble metal nanoparticles is seldom seen. Because of lack of effective protection ability, aggregation and overgrowth of noble metal nanoparticles on PANI have been commonly seen,[27−29] and control over size of noble metal nanoparticles has been limited. As a result, although great achievements have been made in this field, there are still some fundamental questions that need to be solved, such as the effect of doping acid.

Herein, the controllable fabrication of typical gold nanoparticles that evenly deposited on surfaces of PANI nanofibers is reported. It is found that gold nanoparticles that uniformly supported on surfaces of PANI nanofibers can be realized by simply introducing a function doping acid (typical thioglycolic acid (TA)) that shows strong affinity toward gold nanoparticles into PANI nanofibers. Reaction mechanisms involved in redox reaction between PANI and noble metal salts and effects of doping acid on reaction kinetics, size, and uniformity of PANI/noble metal composites are systematically investigated. It is found that size of gold nanoparticles can be tuned ranging from 2 to 10 nm in a controlled manner in the case of TA-doped PANI nanofibers. Formation mechanisms involved have been recommended. This method is also applicable to synthesize uniform PANI nanofiber composites with other noble metal nanoparticles, such as platinum nanoparticles, which shows the diversity of our proposed method for PANI/noble metal nanoparticle composites. Furthermore, PANI nanofiber/gold nanoparticle composites could be used as catalysts with good catalytic activity for

*Corresponding author. E-mail: guorong@yzu.edu.cn.

 Published on Web 11/23/2010

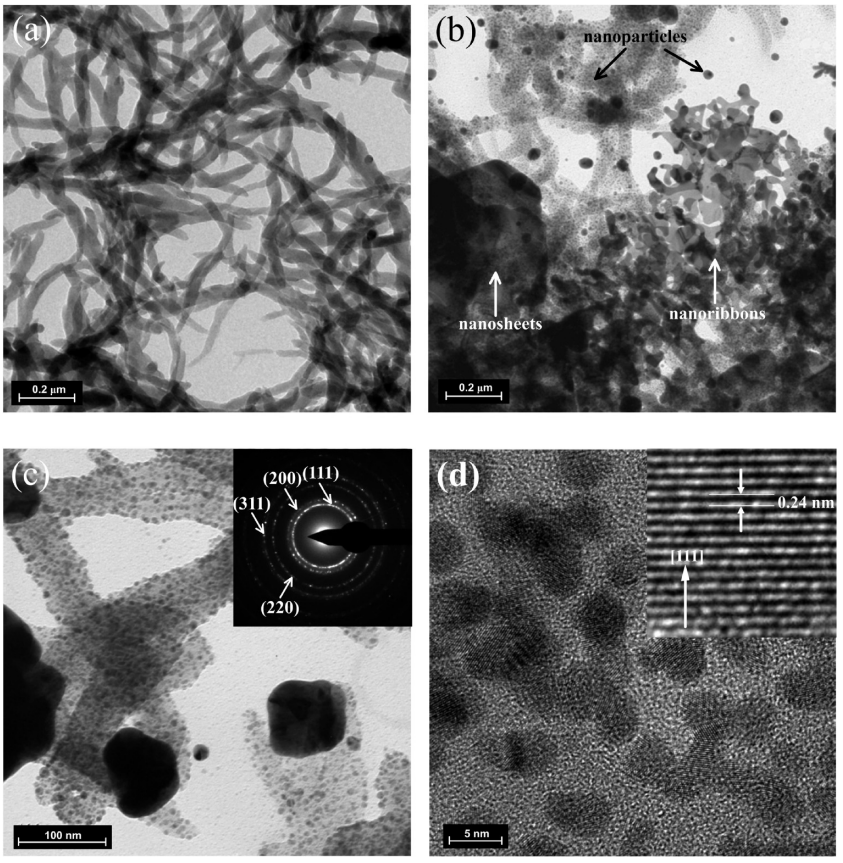

Figure 1. TEM images of (a) PANI nanofibers and (b−d) PANI nanofiber/gold nanoparticle composites. Insets in figure c and d show corresponding ED pattern of PANI nanofiber/gold nanoparticle composites and HR-TEM image of gold nanoparticle, respectively. Synthetic conditions for composites: $[PANI]_{dedoped}$ = 2.0 g/L, $[HAuCl_4]$ = 3.6×10^{-3} mol/L, 2 h, 20 °C.

the reduction of 4-nitrophenol (4NP) in the presence of $NaBH_4$ showing their potential application in catalytic reactions.

2. Materials and Methods

2.1. Chemicals. Aniline monomer (Shanghai Chemical Co.) was distilled under reduced pressure before use. Cetyltrimethylammonium bromide (CTAB), poly(vinylpyrrolidone) (PVP, K-30), and all other reagents of analytical grade purchased from Aldrich were used without further purification. The water used in this study was deionized by Milli-Q Plus system (Millipore, France), having 18.2 MΩ electrical resistivity.

2.2. Synthesis of PANI Nanofibers. Synthesis of PANI nanofibers was according to ref 6: In a typical procedure, 0.3 mL of aniline monomer and 0.18 g of ammonium peroxydisulfate were dissolved in two vials containing 10 mL of 1.0 M HCl. The newly prepared solutions were then poured rapidly into a 30 mL glass vial and shaken vigorously for ~30 s. The mixtures were left still for 2 h. The obtained mixtures were thoroughly purified by deionized water and then excess 0.1 M NH_4OH(aq) for dedoping. After that, products were redispersed in deionized water, or doped in 20 mL of 1.0 M citric acid, camphorsulfonic acid, or TA, and then centrifugated and redispersed in deionized water for further use.

2.3. Synthesis of PANI Nanofiber/Gold Nanoparticle Composite. In a typical synthesis, 0.36 mL of $HAuCl_4$ aqueous solution (0.1 M) was added to 10 mL of PANI nanofibers (2.0 g/L) in one portion. Then the reaction system was maintained under magnetic stirring at room temperature for 2 h. Finally, the products were washed with deionized water and then dried in a vacuum at 60 °C for 24 h.

2.4. $NaBH_4$ Reduction of 4NP Catalyzed by PANI Nanofiber/Gold Nanoparticle Composites. Typically, aqueous solution of $NaBH_4$ (1.0 mL, 1.5×10^{-2} M) was mixed with aqueous 4NP solution (1.7 mL, 2.0×10^{-4} M) in the quartz cell (1 cm path length), leading a color change from light yellow to yellow-green. Then, gold catalysts (0.3 mL, 2.0×10^{-4} M) were added to the mixture and quickly placed in the cell holder of the spectrophotometer. The progress of the conversion of 4NP to 4-aminophenol (4AP) was then monitored via the UV−vis spectroscopy by recording the time-dependent adsorption spectra of the reaction mixture with a time interval of 10 min in a scanning range of 200−700 nm at ambient temperature.

2.5. Characterization. The morphologies of products were examined by a transmission electron microscopy (TEM, Tecnai-12 Philip Apparatus Co.). Fourier transform infrared (FTIR) spectra of products were recorded in the range 400−4000 cm^{-1} using FTIR spectroscopy (Nicolet-740). The sample was prepared in a pellet form with spectroscopic-grade KBr. The X-ray diffraction (XRD) patterns of samples were recorded on a German Bruker AXS D8 ADVANCE X-ray diffractometer. Ultraviolet−visible (UV−vis) spectra (UV-2501, Shimadzu Corp., Japan) of products dispersed in water were measured in the range 250−900 nm. The resulting molar of $AuCl_4^-$ was determined by atomic absorption spectroscopy (AAS) analysis. After formation of gold nanoparticles as precipitation at the bottom of a reaction vessel, the upper transparent solution was analyzed by AAS to confirm the remaining of unreacted raw material of $AuCl_4^-$.

3. Results and Discussion

3.1. Synthesis, Characterization, and Formation Mechanism of PANI Nanofiber/Gold Nanoparticle Composites. Uniform PANI nanofibers are synthesized using the rapid-mixing method as reported where the average diameter is about 50 nm and length is several micrometers, as shown in Figure 1a. As PANI nanofibers as-synthesized are in their

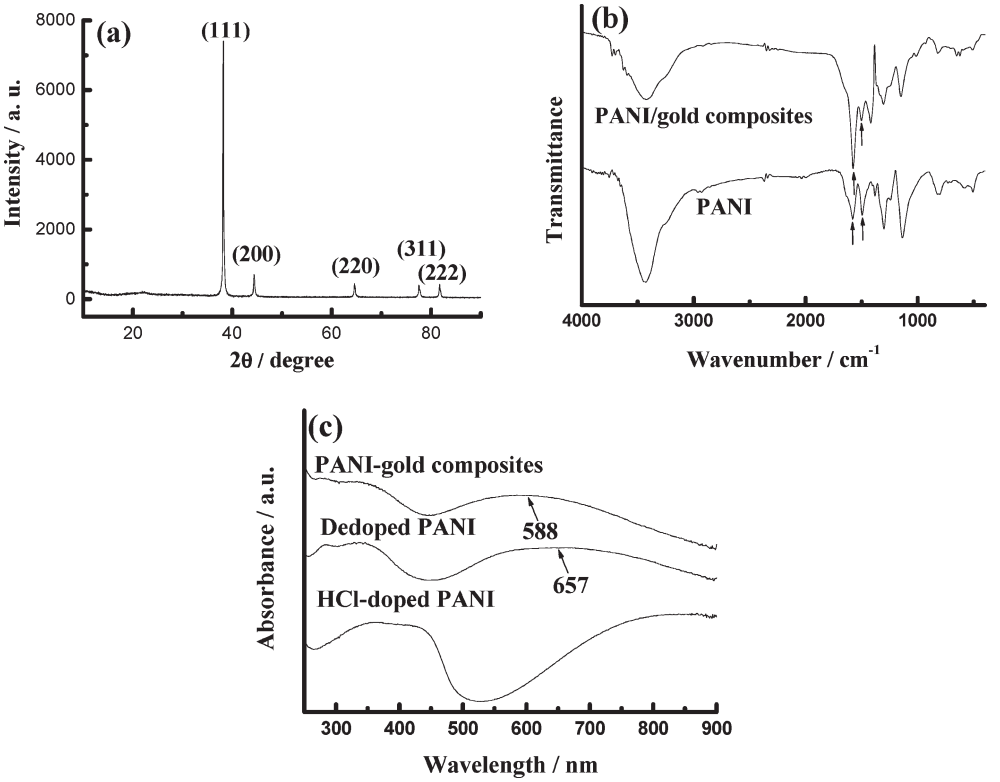

Figure 2. (a) XRD pattern of PANI nanofiber/gold nanoparticle composites. (b) FTIR spectra of PANI nanofibers and PANI nanofiber/gold nanoparticle composites. (c) UV−vis spectra of HCl-doped PANI, dedoped PANI, and PANI nanofiber/gold nanoparticle composites.

doping state, dedoping process of PANI nanofibers with 0.1 M NH_4OH(aq) is applied, and then the obtained dedoped PANI nanofibers are redispersed in aqueous solution. There is no obvious change in size and morphology of PANI nanofibers during dedoping processes as verified by TEM images, which is also consistent with ref 30. Then a certain amount of 0.1 mol/L $HAuCl_4$ aqueous solution is added into aqueous suspension of dedoped PANI nanofibers to initial the redox reaction. After redox reaction between PANI and $HAuCl_4$, gold particles can be observed as shown in Figure 1b, which indicates that gold ions can be reduced to metallic state of gold nanoparticles by dedoped PANI. Different shapes of gold particles apart from PANI nanofibers can be observed as marked in Figure 1b, such as gold nanoparticles (50−100 nm in size), gold nanosheets (~0.5 μm in dimension), and gold nanoribbons (20−50 nm in diameter). Besides, close observation on PANI nanofibers reveals that gold nanoparticles with size of ~5 nm are evenly deposited on surfaces of PANI nanofibers (Figure 1c). Figure 1d shows the high-resolution TEM image, where the clear lattice fringes ~0.24 nm are attributed to the (111) plane of face-centered cubic (fcc) gold, indicating the signal crystal of each gold nanoparticle.[31] The electron diffraction (ED) pattern of PANI nanofiber/gold nanoparticle composite is also shown in inset of Figure 1c, which displays sharp rings indexed to the (111), (200), (220), and (311) planes of fcc gold.

PANI nanofiber/gold nanoparticle composites are further characterized by XRD, FTIR, and UV−vis spectroscopies. As shown in Figure 2a, five obvious main peaks indexed to the (111), (200), (220), (311), and (222) planes of fcc gold,[32] indicating the presence of gold nanoparticles in products. The broad band centered at $2\theta = 20°-30°$ reveals the amorphous feature of PATP polymer. As displayed in Figure 2b, the characteristics for PANI, such as N−H stretching vibrations at 3200−3500 cm^{-1} and C=C stretching deformation of quinonoid and benzenoid rings at 1576 and 1503 cm^{-1}, respectively, are clearly seen. The ratio of the relative intensity of the two peaks is about 1.0, which indicates that similar nitrogen quinonoid and benzenoid ring structures exist in the PANI chains.[33] The band at 1381 cm^{-1}, attributed to a C−N stretching vibration in the neighborhood of a quinonoid ring, is characteristic of dedoped PANI. As for PANI nanofiber/gold nanoparticle composites, it is revealed that the relative intensity of C=C stretching vibrations of quinonoid (1576 cm^{-1}) to benzenoid (1503 cm^{-1}) rings increases significantly after loading gold nanoparticles, indicating PANI is oxidized from emeraldine base to pernigraniline base form, which is also consistent with previous reports.[13,24] Besides, the relatively intensity of peak for N−H stretching vibrations to others decreases markedly, indicating interactions of gold nanoparticles with amine and imine groups in PANI chains. UV−vis spectra of HCl-doped PANI nanofibers are shown in Figure 2c. Doped PANI shows three characteristic absorption bands at about 320−360, 400−420, and ~800 nm wavelengths. The first absorption band arises from $\pi-\pi^*$ electron transition within benzenoid segments. The second and third adsorption bands are related to doping level and formation of polaron, respectively.[34] The first two bands are often combined into a flat or distorted single peak with a local maximum between 360 and 420 nm. It is clearly seen that HCl-doped PANI nanofibers show typical adsorption peaks centered at 368 and 870 nm. The appearance of peak centered at 657 nm that corresponds to the benzenoid to quinonoid excitonic transition indicates the dedoped state of PANI nanofibers. As for the UV−vis spectrum of PANI nanofiber/gold nanoparticle composites, an obvious blue shift of the peak at 657−588 nm indicates the transformation of emeraldine base (dedoped PANI nanofibers) to pernigraniline base (oxidized form of PANI).[1]

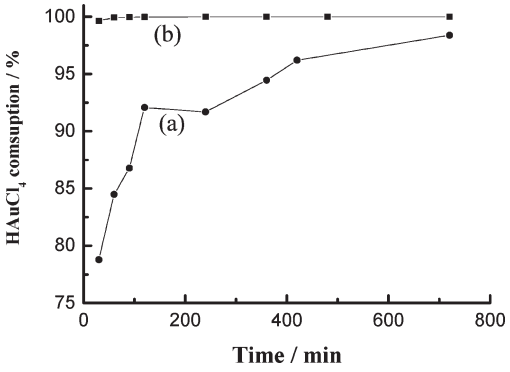

Figure 3. Time-course $HAuCl_4$ consumption during redox reaction between $HAuCl_4$ and (a) dedoped PANI nanofibers or (b) HCl-doped PANI nanofibers.

According to results from FTIR and UV−vis analysis and also ref 22, it is believed that the redox reaction equation between PANI base and $HAuCl_4$ may be as follows:

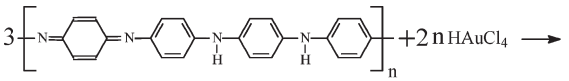

(1)

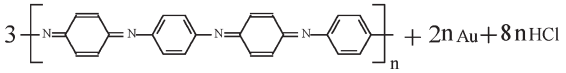

Moreover, it is also found that if excess $HAuCl_4$ is used (conditions of molar ratio of $[HAuCl_4]/[PANI]_{aniline\ unit}$ more than 1:6, eq 1), $HAuCl_4$ that is more than theoretical expectation can be reduced to metallic state of gold nanoparticles. On the basis of the observations, we speculate that, in addition to benzenoid rings, amine groups in PANI main chains should also function as reductant for reduction of $HAuCl_4$.[35,36] Therefore, besides interactions between gold nanoparticles and PANI, consuming of amine groups in PANI main chains during redox reactions may also resulted in decreased intensity of N−H stretching vibrations at 3200−3500 cm^{-1}.

3.2. Effect of Reaction Time, Temperature, and Concentration. The inuniformity of gold nanoparticles and inhomogeneity of composites as clearly seen from Figure 1 may limit their potential applications, possibly due to the obvious difficulty in evaluating morphology- or size-dependent properties. As morphology of PANI nanofibers almost unchanged during synthesis, our following efforts are devoted to improve uniformity of PANI nanofiber/gold nanoparticle composites, mainly the homogeneity and uniformity of gold nanoparticles, by controlling experimental parameters such as reaction time, temperature, and reagent concentration.

During the reaction processes, the $HAuCl_4$ consumption is monitored as shown in Figure 3a, where the yield of gold nanoparticles can achieve more than 90% within 2 h. The time-dependent evolution of products is also recorded by TEM images as displayed in Figure 4. It is found that gold nanosheets, nanoribbons, and large nanoparticles spontaneously formed during early reaction stages (Figure 4a); meanwhile, size of gold nanoparticles supported on PANI nanofibers increases with reaction time (Figure 4a−d). For example, size of gold nanoparticles that supported on PANI nanofibers increases form about 2 to 15 nm when prolonging reaction time from 0.5 to 12 h, respectively. Temperature is also considered, and little effect on resulting morphology is observed (Figure S1).

Concentration of $HAuCl_4$ is found to have a profound effect on resulting morphology. As shown in Figure 5, with

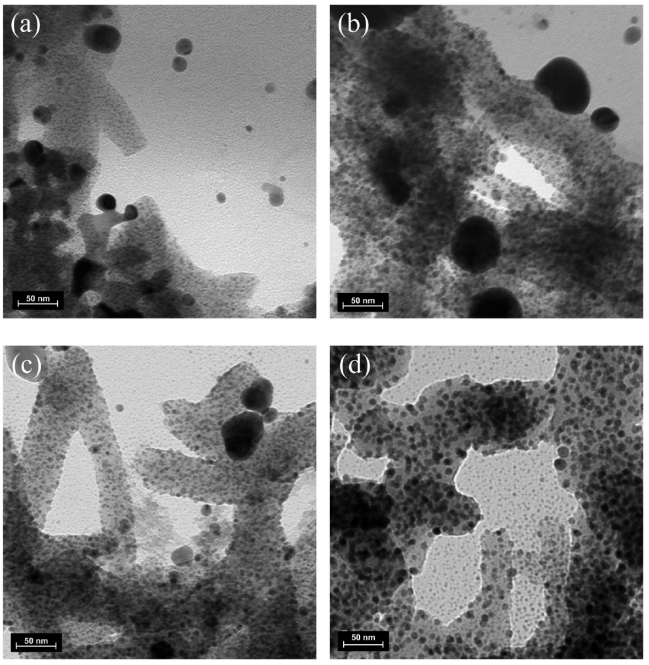

Figure 4. TEM images of PANI nanofiber/gold nanoparticle composites synthesized at different reaction times (h): (a) 0.5, (b) 2, (c) 6, and (d) 12. Synthetic conditions: $[PANI]_{dedoped}$ = 2.0 g/L, $[HAuCl_4]$ = 3.6×10^{-3} mol/L, 20 °C.

$HAuCl_4$ concentration decreases from 1.8×10^{-3} to 7.2×10^{-4} mol/L, it is found that the proportion and density of gold nanoparticles deposited on surfaces of PANI nanofibers decrease, and the proportion of large gold nanoparticles with size of 0.2 μm apart from PANI nanofibers clearly increases (Figure 5a−d). As $HAuCl_4$ concentration further decreases to 3.6×10^{-4} and 1.8×10^{-4} mol/L, bare PANI nanofibers and large gold nanoparticles are evidenced (Figure 5e−h). Then, it is concluded that only aggregated large gold nanoparticles apart from PANI nanofibers can be found under low $HAuCl_4$ concentration, which is unfavorable for gaining uniform PANI nanofiber composites with evenly dispersed gold nanoparticles.

As summarized from these results, it is hard to obtain uniform PANI nanofiber composite with gold nanoparticles evenly deposited by just simply tuning reaction time, temperature, or reagent concentration. According to the generation of gold nanoparticles during synthesis, the redox reaction between polymer and gold salt should happen around surfaces of PANI nanofibers where oxidant and reductant meet together, and finally gold nanoparticles are formed. Because of interactions between gold nuclei with polymer matrix (including amino and benzene groups in PANI that can stabilize gold nanoparticles), gold nanoparticles will be located on surfaces of PANI surfaces. However, it should be noted that besides the contact sites of gold nuclei with polymer matrix, other surfaces are not effectively protected, and then the neighboring gold nuclei will fuse and aggregate which leads to growth and aggregation of gold nanoparticles (Scheme 1).[24]

3.3. Effect of Doping Acid. Recent reports have shown that doped PANI also can react with some noble metal ions (including gold ions) that lead to the formation of metallic noble metals.[13] Comparatively, the $HAuCl_4$ consumption during synthesis when using HCl-doped PANI nanofibers is also monitored, and results are shown in Figure 3b. Results from Figure 3 reveal faster reaction rate and higher yield of gold nanoparticles in the case of HCl-doped PANI

nanofibers as compared with that of dedoped PANI nanofibers. Inspired by these results, we assume that if an acid with functional groups that showing strong affinity to gold nanoparticles is doped to PANI, then the growth and aggregation of gold nuclei will be retarded that leads to formation of gold nanoparticles with smaller size, meanwhile gaining high output of gold nanoparticles. Because of the presence of doping acids on PANI main chains, it is speculated that gold nanoparticles will be evenly deposited on surfaces of PANI nanofibers. Three different doping acids of citric acid, camphorsulfonic acid, and TA are investigated.

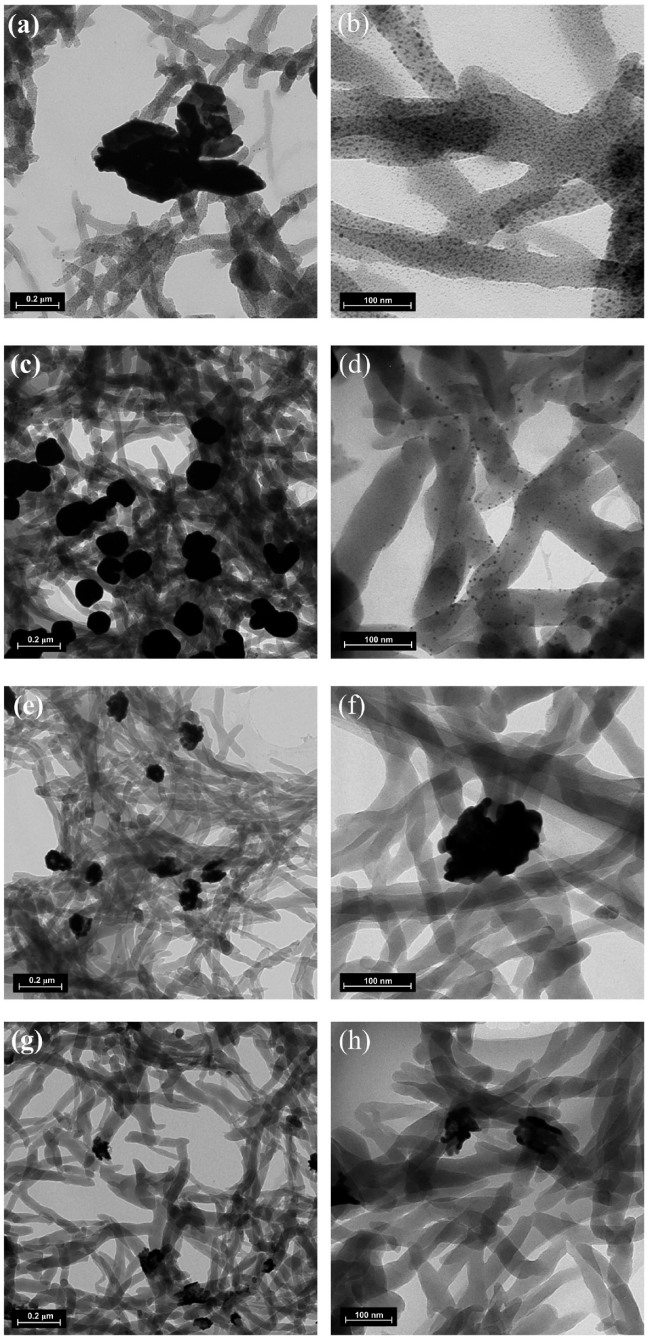

Figure 5. TEM images of PANI nanofiber/gold nanoparticle composites synthesized at different $HAuCl_4$ concentration (mol/L): (a, b) 1.8×10^{-3}, (c, d) 7.2×10^{-4}, (e, f) 3.6×10^{-4}, and (g, h) 1.8×10^{-4}. Synthetic conditions: $[PANI]_{dedoped} = 2.0$ g/L, 2 h, 20 °C.

The doping state of PANI nanofibers should be first claimed. Take TA as an example. It is well-known that change in color is indicative for evaluating doping state of PANI. As shown in Figure 6, HCl-doped PANI nanofibers show characteristic color in green, whereas blue in color is observed for dedoped PANI nanofibers. After redoping with TA, green appearance in color indicates the TA has been doped into PANI nanofibers. In addition, the UV−vis spectrum for TA-doped PANI nanofibers is also conducted as shown in Figure 6b, which shows typical doped state of PANI. Therefore, it is believed that TA has been successfully doped into PANI nanofibers. FTIR spectra of HCl and TA-doped PANI nanofibers are identical with each other as revealed in Figure 6c, indicating that PANI polymer almost maintain the same chemical structures using different doping acids. Furthermore, preliminary experiments show that citric acid, camphorsulfonic acid, or TA alone cannot reduce $HAuCl_4$ into metallic states. Therefore, gold ions should be reduced to metallic state only by PANI after addition of $HAuCl_4$ into doped PANI nanofibers.

As the dopant may change the chemical nature of the PANI nanofibers,[37] morphology of products using HCl-doped PANI nanofibers instead of dedoped PANI nanofibers is also examined. In comparison with the case of dedoped PANI nanofibers (Figure 1), large gold nanoparticles apart from PANI nanofibers are also seen (Figure 7a); however, density of gold nanoparticles deposited on surfaces of PANI nanofibers decreased significantly (Figure 7b). Because of faster reaction kinetics, more gold nuclei are formed during early stage of reaction, and then gold nanoparticle in tens of nanometers instead of larger aggregation of nanosheets and nanoribbons in range of submicrometers are formed. However, due to the presence of HCl in PANI chains, exposure of PANI main chains functional groups of amine and imine groups toward gold nanoparticles decreases and then leads to the decrease of density of gold nanoparticles supported on surfaces of PANI nanofibers. The uniformity of composites has been improved when citric acid-doped PANI nanofibers are used (Figure 7c,d) and becomes better when camphorsulfonic acid-doped PANI nanofibers are chosen (Figure 7e,f). However, gold nanoparticles with size exceeds 100 nm apart from PANI nanofibers are still seen in products, which illustrates that citric acid and camphorsulfonic acid doped in PANI nanofibers cannot effectively protect aggregation of gold nanoparticles.

In the case of TA-doped PANI nanofibers, it is interesting to find that almost all gold nanoparticles are evenly deposited on surfaces of PANI nanofibers, and the uniformity of

Scheme 1. Schematic Illustration for the Formation of PANI Nanofiber/Gold Nanoparticle Composites

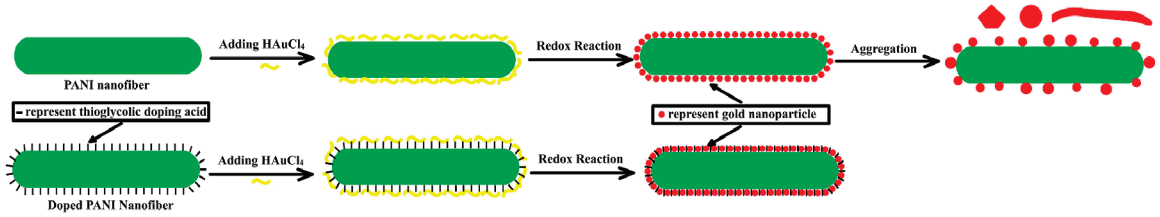

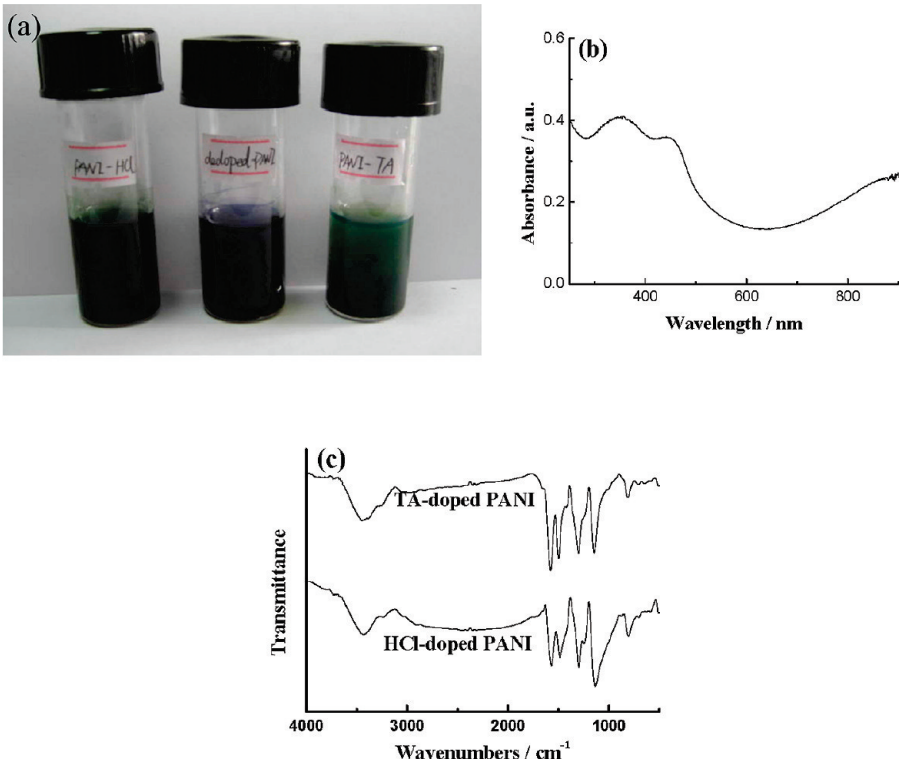

Figure 6. (a) Optical images of HCl-doped, dedoped, and TA-doped PANI nanofibers. (b) UV−vis spectrum of TA-doped PANI nanofibers. (c) FTIR spectrum of HCl and TA-doped PANI nanofibers.

such composite nanofibers is near ~100% (Figure 8). In comparison with Figures 1 and 7a,b where dedoped and HCl-doped PANI nanofibers are used, gold nanoparticles with uniform size of about 10 nm that evenly deposited on surfaces of PANI nanofibers (Figure 8a,b) can be evidenced when TA-doped PANI nanofibers are chosen instead while maintaining other synthetic conditions unchanged. When decreasing $HAuCl_4$ concentration from 3.6×10^{-3} to 1.8×10^{-4} mol/L, it is observed that gold nanoparticles still evenly deposited on surfaces of PANI nanofibers, and the size of gold nanoparticles decreases from ~10 to ~2 nm (Figure 8a−j). Therefore, in comparison with the case of dedpoed PANI used, gold nanoparticles as-formed during early stage of reaction will be located on surfaces of PANI nanofibers, and other surfaces in addition to contact sides will be effectively protected by TA in the case of TA-doped PANI nanofibers as illustrated in Scheme 1. Then it can be concluded that a doping acid that shows strong affinity toward gold nanoparticles introduced to PANI nanofibers will effectively prevent aggregation of gold nanoparticles which leads to formation of uniform composites with gold nanoparticles evenly deposited on surface of PANI nanofibers. A comparative study by using a surfactant instead of doping acid TA is also investigated. It is seen that when using a commonly used cation surfactant CTAB, the size of gold nanoparticles is larger, and most of the gold nanoparticles apart from PANI nanofibers are seen (Figure S2a). In the case of PVP, gold nanoparticles are more uniform; however, gold nanoparticles that keep away from PANI nanofibers are also seen (Figure S2b). Therefore, it is believed that doping acid of TA that doped in PANI nanofibers can effectively stabilize gold nanoparticles on surfaces of PANI nanofibers, which indirectly proves the proposed mechanisms as given in Scheme 1.

3.4. Adaptability for Synthesize Other PANI Nanofiber/Noble Metal Nanoparticle Composites. Instead of gold nanoparticles, this strategy is also applicable to synthesis of other noble metal nanoparticles that evenly deposited on surfaces of PANI nanofibers (Scheme S1). As shown in Figure 9, it is seen that platinum nanoparticle aggregations that apart from PANI nanofibers are mostly seen when using dedoped PANI nanofibers (Figure 9a), whereas platinum nanoparticles that evenly deposited on surfaces of PANI nanofibers (Figure 9b) can be fabricated using TA-doped PANI nanofibers. In the case of silver, it is seen that silver nanoparticles with size of about 50−100 nm can be evidenced when using dedoped PANI nanofibers (Figure 9c), whereas smaller silver nanoparticles (less than 20 nm) deposited on surfaces of PANI nanofibers are observed using TA-doped PANI nanofibers (Figure 9d). However, it is not applicable to palladium nanoparticles where palladium nanoparticles with the same size and distribution can be evidenced regardless of using doped or dedoped PANI nanofibers (Figure S3). This may be related to affinity between doping acids and noble metal nanoparticles.

3.5. Catalytic Activities of PANI Nanofiber/Gold Nanoparticle Composites in the $NaBH_4$ Reduction of 4NP. Catalytic activities of PANI nanofiber/gold nanoparticle composites are examined by choosing a well-known catalysis reaction involving reduction of 4NP to 4AP by $NaBH_4$. In the absence of catalysts, the mixtures of 4NP and $NaBH_4$ show an adsorption band at λ_{max} = 400 nm, corresponding to the 4NP ions in alkaline conditions. This peak remains unaltered with time, indicating that the reduction did not take place in the absence of a catalyst.[38,39] However, the addition of a small amount of PANI nanofiber/gold nanoparticle composites to the above reaction mixture causes fading and ultimate bleaching of the yellow color of the reaction mixture. Since excess $NaBH_4$ was present in the reaction solution and the reduction of 4NP by $NaBH_4$ was negligible in the absence of Au nanoparticles, the reaction could be considered pseudo-first-order with respect to the concentration of 4NP.

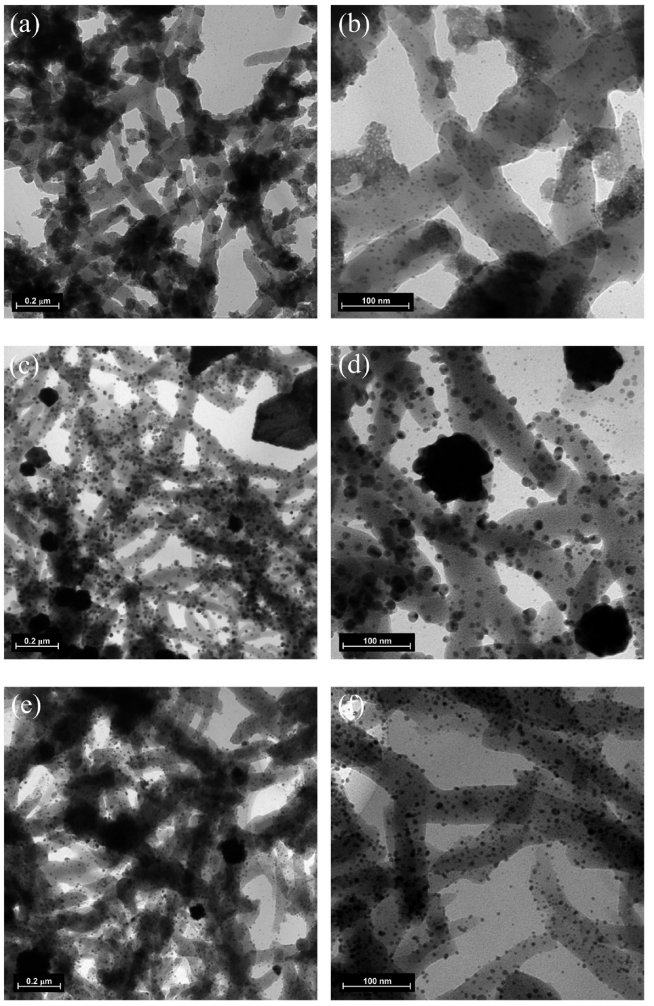

Figure 7. TEM images of PANI nanofiber/gold nanoparticle composites synthesized when PANI nanofibers are doped with different acid: (a, b) citric acid and (c, d) camphorsulfonic acid. Synthetic conditions: $[PANI]_{doped} = 2.0$ g/L, $[HAuCl_4] = 3.6 \times 10^{-3}$ mol/L, 2 h, 20 °C.

PANI nanofiber-supported gold nanoparticles with two different size of 10 nm (Figure 8a,b) and 2 nm (Figure 8i,j) are chosen as catalysts for evaluating the effect of catalyst size on catalytic activity. Time-dependent adsorption spectra of this reaction mixture show the disappearance of the peak at 400 nm that accompanied by a gradual development of a new peak at 300 nm corresponding to the formation of 4AP (Figure 10). It should be noted that catalyst content of gold nanoparticles involved are maintained the same for different sized gold catalysts, and then the content of PANI nanofibers for 2 nm gold nanoparticles is relatively high as compared with 10 nm gold catalysts. Besides, the adsorption spectra after 6 min shifted to less than 400 nm and almost unchanged with increasing reaction time (Figure 10a), which indicates that such adsorptions come from PANI nanofibers. It is seen that the reduction of 4NP to 4AP will be finished within few minutes with gold catalysts of small size (Figure 10a) while that tens of minutes with large size (Figure 10b). As the absorbance of 4NP is proportional to its concentration in the medium, the ratio of absorbance at time t (A_t) to that at $t = 0$ (A_0), i.e., A_t/A_0, could be used as the ratio of concentration of 4NP at time t to that at t_0, i.e., $A_t/A_0 = C_t/C_0$.[40] As shown in Figure 10c, $\ln(C_t/C_0)$ versus time was obtained. Upon the addition of gold nanocatalysts, a certain period of time (defined as t_{ads}) was required for the 4NP to adsorb onto the catalyst's surfaces before reduction could be initiated.[41] As shown in Figure 10a,b, the t_{ads} is about 4 min for 10 nm gold catalysts while it is almost undetectable indicating very fast adsorption process. The

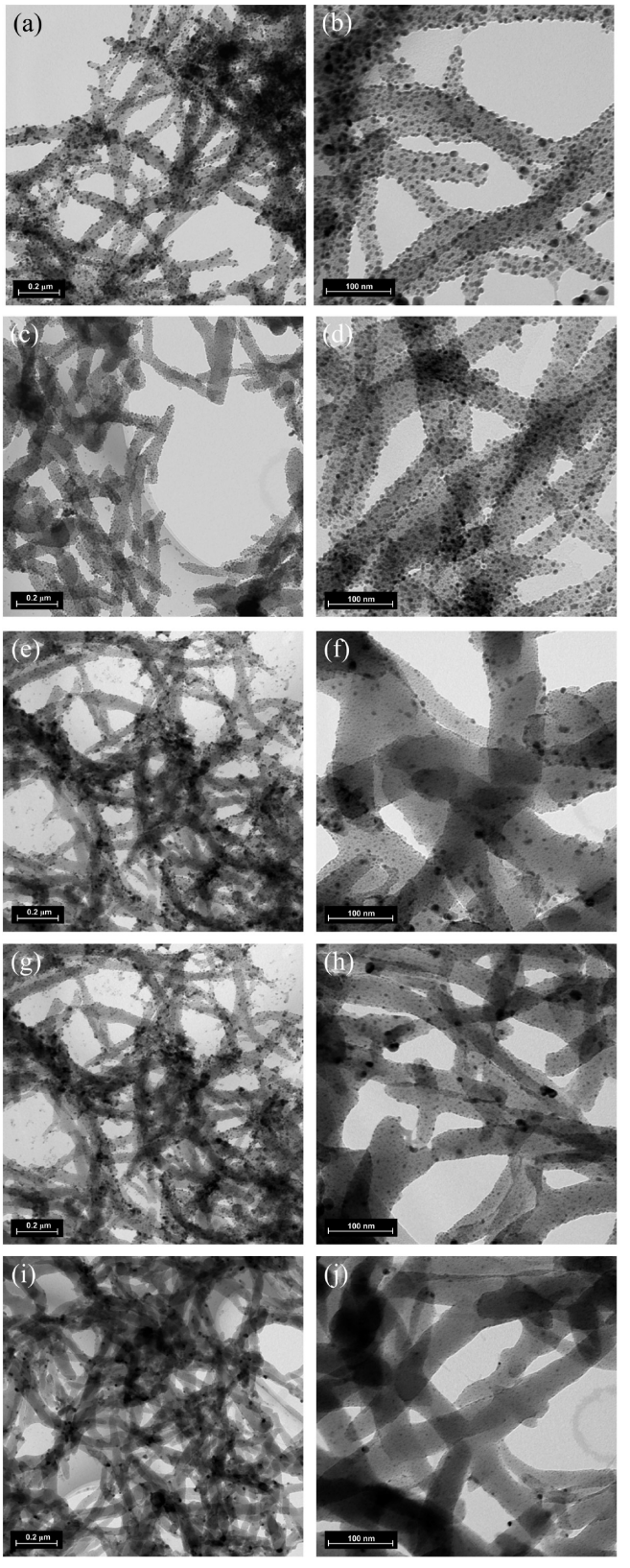

Figure 8. TEM images of PANI nanofiber/gold nanoparticle composites synthesized at different $HAuCl_4$ concentration (mol/L): (a, b) 3.6×10^{-3}, (c, d) 1.8×10^{-3}, (e, f) 7.2×10^{-4}, (g, h) 3.6×10^{-4}, and (i, j) 1.8×10^{-4}. Synthetic conditions: $[PANI]_{TA\ doped} = 2.0$ g/L, 2 h, 20 °C.

kinetic reaction rate constant (defined as k_{app}) is also estimated from the linear relationship, which is 11.7×10^{-3} and 2.5×10^{-3} s^{-1} for gold nanoparticles with size of 2 and 10 nm, respectively. It is seen that the reaction catalyzed by smaller gold nanoparticles (2 nm) shows the shorter adsorption time and faster reaction rate.

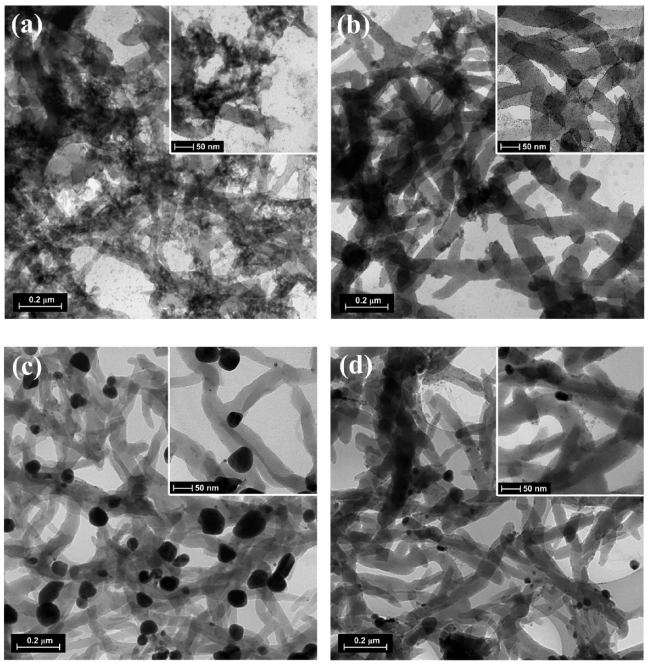

Figure 9. TEM images of (a, b) PANI nanofiber/platinum nanoparticle and (c, d) PANI nanofiber/silver nanoparticle composites synthesized with (a, c) dedoped and (b, d) TA-doped PANI nanofibers. Synthetic conditions: [PANI] = 2.0 g/L, $[H_2PtCl_6] = 2.7 \times 10^{-3}$ mol/L, $[AgNO_3] = 1.1 \times 10^{-2}$ mol/L, 2 h, 20 °C.

It is known that the reusability is the main advantage of using heterogeneous catalyst rather than homogeneous catalyst. As a result, the reusability of PANI nanofiber-supported gold nanoparticles as catalyst toward the reduction of 4NP in the presence of $NaBH_4$ is investigated. The catalysts are recovered by simple centrifugation after completion of the first cycle and then washed with water and reused in the next cycle. Results confirm that PANI nanofiber-supported gold nanoparticles can be used as recycled catalysts involved in reduction of 4NP, where the catalytic reaction time increase with cycles. The k_{app} in six cycles for the reduction of 4NP in the presence of $NaBH_4$ with 2 nm gold nanoparticles are given in Table 1. The decreased catalytic activity with increasing cycles may result from loss of catalysts during centrifugation and purification processes of catalysts.[24,39]

4. Summary

Gold nanoparticles with controllable size that evenly supported on PANI nanofibers have been fabricated through redox activity of PANI nanofibers toward $HAuCl_4$. It is found that gold nanoparticles will be evenly deposited on surfaces of PANI nanofibers when a doping acid that show strong affinity toward gold nanoparticles, such as thioglycolic acid, is introduced to PANI nanofibers. By changing concentration of $HAuCl_4$, the size of gold nanoparticles that can be tuned ranges from 10 to 2 nm, while maintaining high uniformity of composites. It is also shown the successful synthesis of platinum and silver nanoparticles evenly supported on PANI nanofibers, which demonstrates the diversity of our proposed method for PANI nanofiber/noble

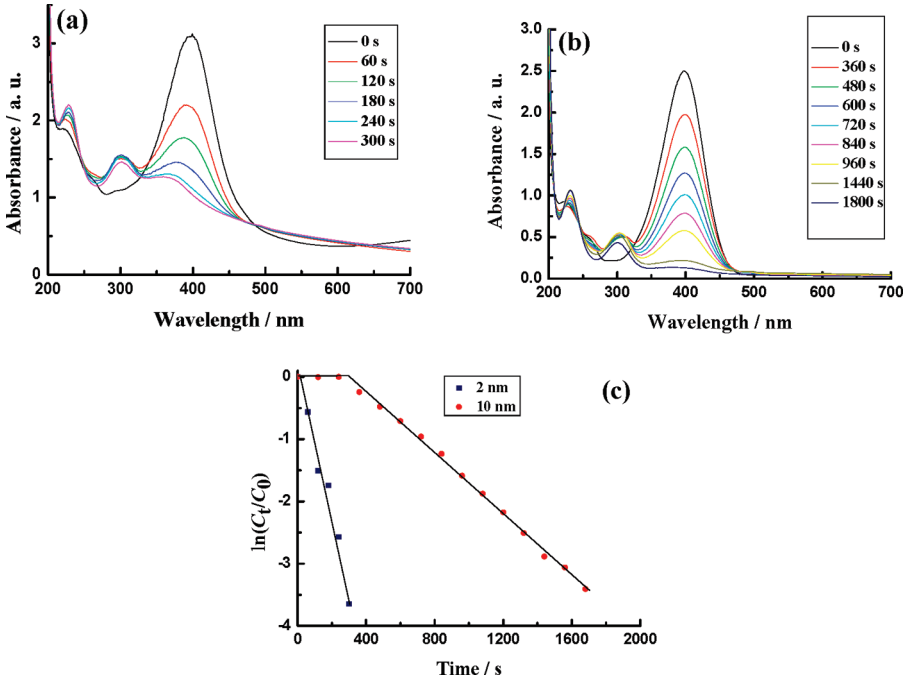

Figure 10. Successive UV−vis adsorption spectra of the reduction of 4NP by $NaBH_4$ in the presence of (a) 2 nm and (b) 10 nm gold nanoparticles supported on PANI nanofibers as imaged in Figure 8. (c) Plot of $\ln(C_t/C_0)$ of 4NP against time for the gold nanoparticles with different size.

Table 1. k_{app} in Different Cycles of Catalytic Reduction of 4NP in the Presence of $NaBH_4$ with PANI Nanofiber-Supported Gold Nanoparticles Catalyst (Gold Size: 2 nm)

use	first	second	third	fourth	fifth	sixth
k_{app} (s^{-1})	11.7×10^{-3}	6.2×10^{-3}	5.5×10^{-3}	5.1×10^{-3}	3.7×10^{-3}	3.0×10^{-3}

metal nanoparticle composites. We believe that PANI with other morphologies or other conducting polymers that show redox activity toward noble metal ions may be also applicable for making uniform noble metal nanoparticles/conducting polymer composites upon introducing an appropriate functional doping acid in the conducting polymer matrix. PANI nanofiber/noble metal nanoparticle composites show good catalytic activities and reusability toward the reduction of 4NP in the presence of $NaBH_4$, where the reaction catalyzed by smaller gold nanoparticles (2 nm) shows the shorter adsorption time and faster reaction rate. It is believed that PANI nanofiber/noble metal nanoparticle composites as-synthesized will find promising applications in fields such as catalysis, biosensors, and memory devices, which will be our continuing interest.

Acknowledgment. Funding is acknowledged from the National Natural Scientific Foundation of China (No. 20903079, 21073156, 20773106, and 20633010).

Supporting Information Available: TEM images of gold and palladium composites with PANI nanofibers. This material is available free of charge via the Internet at http://pubs.acs.org.

References and Notes

(1) Kang, E. T.; Neoh, K. G.; Tan, K. L. *Prog. Polym. Sci.* **1998**, *23*, 277–324.
(2) Hatchett, D. W.; Josowicz, M. *Chem. Rev.* **2008**, *108*, 746–769.
(3) Bhadra, S.; Khastgir, D.; Singha, N. K.; Lee, J. H. *Prog. Polym. Sci.* **2009**, *34*, 783–810.
(4) Li, D.; Huang, J.; Kaner, R. B. *Acc. Chem. Res.* **2009**, *42*, 135–145.
(5) Huang, J.; Kaner, R. B. *Angew. Chem., Int. Ed.* **2004**, *43*, 5817–5821.
(6) Li, D.; Kaner, R. B. *J. Am. Chem. Soc.* **2006**, *128*, 968–975.
(7) Chiou, N. R.; Epstein, A. J. *Adv. Mater.* **2005**, *17*, 1679–1683.
(8) Huang, J.; Virji, S.; Weiller, B. H.; Kaner, R. B. *J. Am. Chem. Soc.* **2003**, *125*, 314–315.
(9) Zhang, X. Y.; Goux, W. J.; Manohar, S. K. *J. Am. Chem. Soc.* **2004**, *126*, 4502–4503.
(10) Virji, S.; Huang, J.; Kaner, R. B.; Weiller, B. H. *Nano Lett.* **2004**, *4*, 491–496.
(11) Tseng, R. J.; Huang, J.; Ouyang, J.; Kaner, R. B.; Yang, Y. *Nano Lett.* **2005**, *6*, 1077–1080.
(12) Gao, Y.; Chen, C. A.; Gau, H. M.; Bailey, J. A.; Akhadov, E.; Williams, D.; Wang, H. L. *Chem. Mater.* **2008**, *20*, 2839–2844.
(13) Shih, H. H.; Williams, D.; Mack, N. H.; Wang, H. L. *Macromolecules* **2009**, *42*, 14–16.
(14) Gallon, B. J.; Kojima, R. W.; Kaner, R. B.; Diaconescu, P. L. *Angew. Chem., Int. Ed.* **2007**, *46*, 7251–7254.
(15) Santhosh, P.; Gopalan, A.; Lee, K. P. *J. Catal.* **2006**, *238*, 177–185.
(16) Xu, Q.; Leng, J.; Li, H.; Lu, G.; Wang, Y.; Hu, X. *React. Funct. Polym.* **2010**, *70*, 663–668.
(17) Ozdemir, C.; Yeni, F.; Odaci, D.; Timur, S. *Food Chem.* **2010**, *119*, 380–385.
(18) Feng, Y.; Yang, T.; Zhang, W.; Jiang, C.; Jiao, K. *Anal. Chim. Acta* **2008**, *616*, 144–151.
(19) Corbierre, M. K.; Cameron, N. S.; Sutton, M.; Mochrie, S. G. J.; Lurio, L. B.; Ruhm, A.; Lennox, R. B. *J. Am. Chem. Soc.* **2001**, *123*, 10411–10412.
(20) Wang, J.; Neoh, K. G.; Kang, E. T. *J. Colloid Interface Sci.* **2001**, *239*, 78–86.
(21) Guo, S.; Dong, S.; Wang, E. *Small* **2009**, *5*, 1869–1876.
(22) Seděnkoá, I.; Trchová, M.; Stejskal, J.; Proke, J. *ACS Appl. Mater. Interfaces* **2009**, *1*, 1906–1912.
(23) Han, J.; Liu, Y.; Guo, R. *Adv. Funct. Mater.* **2009**, *19*, 1112–1117.
(24) Han, J.; Liu, Y.; Li, L.; Guo, R. *Langmuir* **2009**, *25*, 11054–11060.
(25) Huang, C. C.; Wen, T. C.; Wei, Y. *Mater. Chem. Phys.* **2010**, *122*, 392–396.
(26) Guo, S.; Dong, A.; Wang, E. *Small* **2009**, *5*, 1869–1876.
(27) Wang, H. L.; Li, W.; Jia, Q. X.; Akhadov, E. *Chem. Mater.* **2007**, *19*, 520–525.
(28) Gao, Y.; Chen, C. A.; Gau, H. M.; Bailey, J. A.; khadov, E.; Williams, D.; Wang, H. L. *Chem. Mater.* **2008**, *20*, 2839–2844.
(29) Xu, P.; Han, X.; Wang, C.; Zhang, B.; Wang, X.; Wang, H. L. *Macromol. Rapid Commun.* **2008**, *29*, 1392–1397.
(30) Huang, J.; Kaner, R. B. *J. Am. Chem. Soc.* **2004**, *126*, 851–855.
(31) Zhang, T.; Wang, W.; Zhang, D.; Zhang, X.; Ma, Y.; Zhou, Y.; Qi, L. *Adv. Funct. Mater.* **2010**, *20*, 1152–1160.
(32) Wang, Y.; Liu, Z.; Han, B.; Sun, Z.; Huang, Y.; Yang, G. *Langmuir* **2005**, *21*, 833–836.
(33) Han, J.; Liu, Y.; Guo, R. *J. Polym. Sci., Part A: Polym. Chem.* **2008**, *46*, 740–746.
(34) Stejskal, J.; Kratochvil, P.; Radhakrishnan, N. *Synth. Met.* **1993**, *61*, 225–231.
(35) Li, X.; Liu, R.; Huang, M. *Chem. Mater.* **2005**, *17*, 5411–5419.
(36) Li, X.; Ma, X.; Sun, J.; Huang, M. *Langmuir* **2009**, *25*, 1675–1684.
(37) Xu, P.; Mack, N. H.; Jeon, A. H.; Doorn, S. K.; Han, X.; Wang, H. L. *Langmuir* **2010**, *26*, 8882–8886.
(38) Liu, J.; Qin, G.; Raveendran, P.; Ikushima, Y. *Chem.—Eur. J.* **2006**, *12*, 2131–2138.
(39) Rashid, M. H.; Mandal, T. K. *Adv. Funct. Mater.* **2008**, *18*, 2261–2271.
(40) Huang, T.; Meng, F.; Qi, L. *Langmuir* **2009**, *113*, 13636–13642.
(41) Zeng, J.; Zhang, Q.; Chen, J.; Xia, Y. *Nano Lett.* **2010**, *10*, 30–35.